

Influence of the radio frequency ponderomotive force on anomalous impurity transport in tokamaks

H. Nordman,¹ R. Singh,² T. Fülöp,¹ L.-G. Eriksson,³ R. Dumont,³ J. Anderson,⁴ P. Kaw,² P. Strand,¹ M. Tokar,⁵ and J. Weiland¹

¹Department of Radio and Space Science, Chalmers University of Technology, Euratom-VR Association, SE-412 96 Göteborg, Sweden

²Institute for Plasma Research, Bhat, Gandhinagar-382 428, India

³Association Euratom-CEA, CEA/DSM/IRFM CEA-Cadarache, France

⁴Department of Applied Mathematics, University of Sheffield, Hicks Building, Hounsfield Road, S3 7RH Sheffield, United Kingdom

⁵Institute for Plasma Physics, Forschungszentrum Jülich GmbH, Association FZJ-Euratom, 52425, Jülich, Germany

(Received 30 January 2008; accepted 21 March 2008; published online 30 April 2008)

Trace impurity transport in tokamaks is studied using an electrostatic, collisionless fluid model for ion-temperature-gradient and trapped-electron mode driven turbulence in the presence of radio frequency (rf) fields, and the results are compared with neoclassical predictions. It is shown that the inward impurity convective velocity (pinch) that is usually obtained can be reduced by the rf fields, in particular close to the wave resonance location where the rf ponderomotive force may be significant. However, the impurity diffusivity and convective velocity are usually similarly affected by the ponderomotive force, and hence the steady-state impurity density peaking factor $-\nabla n_z/n_z$ is only moderately affected by the rf fields. © 2008 American Institute of Physics.

[DOI: [10.1063/1.2908354](https://doi.org/10.1063/1.2908354)]

I. INTRODUCTION

Impurities may have a significant effect on tokamak performance by their contribution to radiation losses and plasma dilution resulting in lower fusion power. In particular, high-Z impurity accumulation, which is observed in many tokamak experiments and is predicted by collisional transport theory,¹ can be detrimental for fusion experiments. Recent experiments^{2–7} have shown that auxiliary heating can influence impurity accumulation. For example, in ASDEX-Upgrade⁸ it has been observed that dominant electron heating via electron cyclotron resonance frequency (ECRF) heating decontaminates the plasma more efficiently than dominant ion heating via ion cyclotron resonance frequency (ICRF) heating.² In DIII-D,⁹ it has been found that application of ECRF is effective in flattening both the electron and the nickel density profile.⁷ In JET,¹⁰ it has been observed that with the addition of ion cyclotron resonance heating to neutral beam heated discharges, accumulation of high-Z impurities can be avoided if most of the heating power is deposited on the electrons, while if the heating is deposited on the ions, the impurities accumulate in the center.^{3,5,6} Hence, it seems possible to avoid the impurity accumulation by choosing the proper amount and type of auxiliary heating. The physical mechanism by which the change of the direction of the impurity convective velocity (pinch) occurs has not yet been clearly identified. The theoretical understanding of these observations is extremely important for the success of the next generation of fusion experiments. A possible explanation for the reversal of the impurity convective velocity is that the electron heating results in the dominance of transport driven by trapped electron (TE) mode turbulence, which may give an outward

convection.¹¹ However, numerical results indicate that for the TE mode instability to be dominant, the normalized ion temperature scale length has to be about a factor of 2 smaller than experimentally observed.⁵

In the present paper, the influence of rf waves in the ion cyclotron range of frequencies on turbulent transport of trace impurities is studied. An electrostatic, collisionless fluid model^{12,13} is used for the description of the trace impurity species as well as for the background turbulence driven by ion temperature gradient (ITG) and TE modes. The turbulence is affected by the ponderomotive force associated with the rf field of the fast magnetosonic wave in the plasma. For the purpose of ICRF heating, this wave is normally launched by antennas located on the low-field side of the tokamak, and for heating scenarios where the wave is strongly damped, such as hydrogen minority heating in a deuterium plasma (H)D, the wave tends to be highly focused to a point near the magnetic axis (see, e.g., Ref. 14). Consequently, for such scenarios strong gradients of the wave field amplitude are expected in the vicinity of the cyclotron resonance of the resonating species, where the wave field decreases strongly in the negative major radius direction due to the absorption ($d|E_{\perp}|^2/dR < 0$). However, it should be noted that also regions with $d|E_{\perp}|^2/dR > 0$ are possible if the cyclotron resonance is on the high-field side of the focal point for the wave. This is illustrated in Fig. 1, where $|E_{\perp}|^2$ of the ICRF wave field in the equatorial midplane is shown as a function of the major radius for parameters typical for the JET tokamak. The wave field was simulated with the EVE code,¹⁵ and the square of the field is given per megawatt (MW) of absorbed ICRF power. As observed, the ponderomotive force ($\sim d|E_{\perp}|^2/dr$) may be large in the vicinity of the resonance location. Earlier

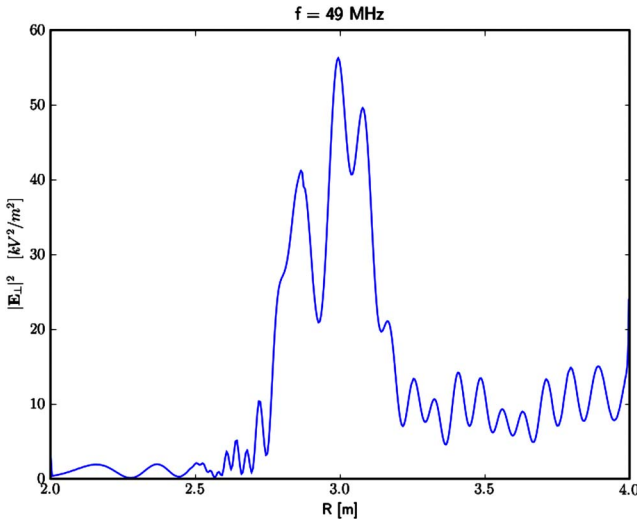


FIG. 1. (Color online) Simulated squared magnitude of the perpendicular electric field in the equatorial midplane for ICRF hydrogen minority heating in deuterium plasma (H)D for a typical JET case. The main parameters of the simulation were as follows: $n_e = 4 \times 10^{19} \text{ m}^{-3}$, $n_H/n_D = 5\%$, $B_0 = 2.8 \text{ T}$, $f_{\text{ICRF}} = 47 \text{ MHz}$. The hydrogen cyclotron resonance location was about 30 cm on the high-field side of the magnetic axis. The square of the field is given for 1 MW of absorbed power, and it is linear in power.

theoretical work¹⁶ has shown that the ponderomotive force may cause a strong modification of the s - α stability diagram for ballooning modes in tokamaks. Here, we show that also the impurity transport may be affected.

The remainder of the paper is organized as follows. In Sec. II, the models used to describe the ITG/TE stability and trace impurity transport are described. Section III discusses the effect of the rf ponderomotive force on the impurity transport. Finally, the conclusions are given in Sec. IV.

II. FORMULATION

To describe the background ITG/TE mode turbulence, a set of fluid equations¹² is used for the particle density n , parallel velocity v_{\parallel} , and temperature T in the presence of an rf ponderomotive force,

$$\frac{\partial n_j}{\partial t} + \nabla \cdot (n_j \vec{v}_j) = 0, \quad (1)$$

$$m_i n_i \frac{\partial \vec{v}_{\parallel i}}{\partial t} + \nabla_{\parallel} p_i + n_i e \nabla_{\parallel} \phi = 0, \quad (2)$$

$$\frac{3}{2} n_j \frac{dT_j}{dt} + n_j T_j \nabla \cdot \vec{v}_j + \nabla \cdot \vec{q}_j = 0, \quad (3)$$

where $j=i, et$ represents ions and trapped electrons, m_i is the ion mass, ϕ is the electrostatic potential, and the perpendicular velocity is $\vec{v}_{\perp} = \vec{v}_E + \vec{v}_* + \vec{v}_p + \vec{v}_{\pi} + \vec{v}_{i-\text{RF}}$, where \vec{v}_E is the $E \times B$ drift, \vec{v}_* is the diamagnetic drift, \vec{v}_p is the polarization drift, \vec{v}_{π} is the stress tensor drift, and \vec{q} is the diamagnetic heat flux. Here, $\vec{v}_{i-\text{RF}}$ is an additional poloidal ion drift caused by the radial rf ponderomotive force, and the convective derivative is defined as $d/dt = \partial/\partial t + \vec{v} \cdot \nabla$. The collisionless electrostatic limit is considered, and the free electrons

are assumed to be Boltzmann-distributed. The ion and electron perturbations are coupled through the quasineutrality condition $\delta n_i/n_i = f_t \delta n_{ei}/n_{ei} + (1-f_t) \delta n_{ef}/n_{ef}$, where f_t is the fraction of trapped electrons. A semilocal analysis^{13,17} is used where the eigenvalue equation is reduced to a set of coupled algebraic equations by assuming a strongly ballooning eigenfunction ($\phi = 1/\sqrt{3\pi}(1+\cos\theta), |\theta| < \pi$). In the treatment of the ion drift due to the ponderomotive force, the compression effect fulfills $\nabla \cdot (\vec{v}_{i-\text{RF}}) \ll \vec{v}_{i-\text{RF}} \cdot \nabla$ and has been omitted. It is clear from the above equations that the main effect of the ponderomotive force ($\vec{k} \cdot \vec{v}_{i-\text{RF}}$) is a shift in the real frequency of the ITG mode. This frequency shift can significantly modify the phase relation between the impurity density and potential perturbations and hence affect the impurity flux.

The trace impurity species is described by the same set of fluid equations¹³ (but neglecting effects of finite impurity Larmor radius), including the effects of the ponderomotive force and parallel impurity compression,

$$(\bar{\omega} - \bar{\Omega}_{z-\text{RF}} + \tau_z^*) \tilde{n}_z - (\varepsilon_{nz} - 1) \tilde{\phi} + \tau_z^* \tilde{T}_z - \frac{k \delta v_{\parallel z}}{\omega_{De}} = 0, \quad (4)$$

$$(\bar{\omega} - \bar{\Omega}_{z-\text{RF}} - 2\tau_z^*) \frac{k \delta v_{\parallel z}}{\omega_{De}} = \frac{Z}{A_z q_*^2} \tilde{\phi} + \frac{\tau_z}{A_z q_*^2} (\tilde{n}_z + \tilde{T}_z), \quad (5)$$

$$(\bar{\omega} - \bar{\Omega}_{z-\text{RF}} + \frac{5}{3} \tau_z^*) \tilde{T}_z - (\varepsilon_{Tz} - \frac{2}{3} \varepsilon_{nz}) \tilde{\phi} - \frac{2}{3} (\bar{\omega} - \bar{\Omega}_{z-\text{RF}}) \tilde{n}_z = 0. \quad (6)$$

Here $\tilde{\phi} = e\phi/T_e$ is the normalized potential and $\tilde{n}_z = \delta n_z/n_z$, $\delta v_{\parallel z}$, and $\tilde{T}_z = \delta T_z/T_z$ are the impurity density, parallel velocity, and temperature perturbations, $\bar{\omega}$ and \vec{k} are the normalized eigenvalue and wave vector of the unstable ITG/TE modes, the overbar denotes normalization with respect to the electron magnetic drift frequency ω_{De} , $\tau_z^* = T_z/ZT_e$, $\tau_z = T_z/T_e$, $\varepsilon_{nz} = -R \partial \ln n_z / 2 \partial r$, $\varepsilon_{Tz} = -R \partial \ln T_z / 2 \partial r$, $A_z = m_z/m_i$, Z is the impurity charge, m_z is the impurity mass, $q_* = 2qk_B\rho_s$ with $\rho_s = c_s/\Omega_{ci}$, and $c_s = \sqrt{T_e/m_i}$. The radial ponderomotive force enters in the impurity equations through the normalized drift frequency $\bar{\Omega}_{z-\text{RF}} = (R/2Zc_z^2) \langle \tilde{v}_{z-\text{RF}} \rangle^2 / \partial r$, where $\tilde{v}_{z-\text{RF}}$ is the radial impurity velocity perturbation at the ICRF wave scale, $\langle \dots \rangle$ is the average over the fast ion cyclotron time scale, and $c_z = \sqrt{T_z/m_Z}$. The term proportional to $2\tau_z^*$ on the left-hand side of Eq. (5) corresponds to curvature effects from $\vec{\nabla} \cdot \vec{\pi}_z$ (the stress tensor). For $T_i/T_e \approx T_z/T_e \approx 1$, the ratio of the radial ponderomotive force experienced by the ion and impurity species is $\bar{\Omega}_{i-\text{RF}}/\bar{\Omega}_{z-\text{RF}} \approx Z$ since the rf velocity field oscillations in the ion and impurity fluid are typically $\tilde{v}_{i-\text{RF}} \approx c_s$ and $\tilde{v}_{z-\text{RF}} \approx c_{sz}$, respectively. Thus, we can neglect the radial ponderomotive effects in the impurity dynamics for $Z \gg 1$. Moreover, for $Z \gg 1$, the ion pressure perturbations in the parallel impurity dynamics [Eq. (5)] can also be neglected. Combining Eqs. (4)–(6), the relation between \tilde{n}_z and $\tilde{\phi}$ can be written as

$$\tilde{n}_z = \left\{ \bar{\omega}(\varepsilon_{nz} - 1) - \tau_z^* \left(\varepsilon_{Tz} - \frac{7}{3} \varepsilon_{nz} + \frac{5}{3} \right) + \frac{Z}{A_z q_*^2} \left(\frac{\bar{\omega} + 5\tau_z^*/3}{\bar{\omega} - 2\tau_z^*} \right) \right\} \frac{\tilde{\phi}}{N}, \quad (7)$$

where $N = \bar{\omega}^2 + (10\tau_z^*/3)\bar{\omega} + (5\tau_z^{*2}/3)$. From the impurity density response, the impurity particle flux can be calculated as $\Gamma_{nz} = -n_z \rho_s c_s \langle \tilde{n}_z (\partial \tilde{\phi} / r \partial \theta) \rangle = -D_z \nabla n_z + n_z V_z$, where D_z and V_z are the impurity diffusivity and convective velocity, respectively,

$$\begin{aligned} \frac{\Gamma_{nz}}{n_z c_s} = & \frac{k_\theta \rho_s \bar{\gamma} |\tilde{\phi}_k|^2}{|N|^2} \left[\varepsilon_{nz} \left(|\bar{\omega}|^2 + \frac{14\tau_z^*}{3} \bar{\omega}_r + \frac{55\tau_z^{*2}}{9} \right) - \varepsilon_{Tz} \left(2\tau_z^* \bar{\omega}_r + \frac{5\tau_z^{*2}}{3} \right) - \left(|\bar{\omega}|^2 + \frac{10\tau_z^*}{3} \bar{\omega}_r + \frac{35\tau_z^{*2}}{9} \right) \right. \\ & \left. + \frac{Z}{A_z q_*^2 |N_1|^2} \left(\tau_z^* \left(\frac{19}{3} \bar{\omega}_r^2 - \frac{1}{3} \bar{\gamma}^2 + \frac{100\tau_z^*}{9} \bar{\omega}_r - 5\tau_z^{*2} \right) + 2\bar{\omega}_r |\bar{\omega}|^2 \right) \right], \end{aligned} \quad (8)$$

where $N_1 = \bar{\Omega} - 2\tau_z^*$. In Eq. (8), the first term is the diffusive flux and the other terms represent the impurity convective velocity with contributions from ∇T_z (thermodiffusive flux), curvature, and parallel impurity compression. We note that the impurity flux given by Eq. (8) is in agreement with the analytical expressions given in Ref. 11 in the relevant limit [see Eqs. (5)–(8) of Ref. 11].

III. INFLUENCE OF THE PONDEROMOTIVE FORCE

The trace impurity diffusivity D_z and convective velocity V_z are calculated from Eq. (8) with the ITG/TE mode eigenvalues taken from Eqs. (1)–(3) for a fixed length scale of the turbulence with $k_\theta^2 \rho_s^2 = 0.1$, and with the potential fluctuation level¹² $|\phi_k| = (\gamma / \omega_{*e})(1/k_\theta L_{ne})$. In Fig. 2, the calculated impurity diffusion coefficient D_z , convective velocity RV_z (in units of $2\rho_s^2 c_s / R$), and normalized impurity density peaking factor $-RV_z / D_z = -R \nabla n_z / n_z$ (assuming a source-free plasma with $\Gamma_{nz} = -D_z \nabla n_z + n_z V_z = 0$) of a trace impurity species as a function of the rf ponderomotive force term $\bar{\Omega}_{i-RF}$ are shown.

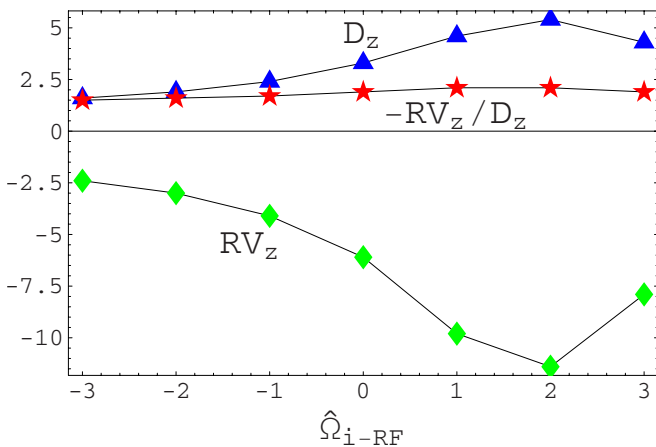


FIG. 2. (Color online) Impurity diffusion coefficient D_z , impurity convective velocity RV_z (in units of $2\rho_s^2 c_s / R$), and normalized impurity density peaking factor $-RV_z / D_z$ as a function of the ICRF ponderomotive force term $\bar{\Omega}_{i-RF}$ for an ITG mode dominated case. The parameters are $R/L_{Tj} = 7$, $Z = 6$, $f_i = 0.5$, $q = 1.4$, $s = 0.8$, $T_e / T_{i,z} = 1$, and $R/L_{ne} = 3$.

The parameters are $R/L_{Ti} = R/L_{Tz} = R/L_{Te} = 7$ (where $R/L_j = -Rdj/dr/j$), $Z = 6$, $f_i = 0.5$, $q = 1.4$ is the safety factor, $s = 0.8$ is the magnetic shear, $T_e / T_{i,z} = 1$, and $R/L_{ne} = 3$. For these parameters, the ITG mode is the dominant instability. For $\bar{\Omega}_{i-RF} < 0$ (corresponding to a situation with $d|E_\perp|^2/dr < 0$) and $\bar{\Omega}_{i-RF} > 2$, a significant reduction of the inward impurity velocity $|V_z|$ is obtained. This is mainly caused by the shift in the ITG real frequency by the ponderomotive force drift. Transiently, this could lead to a reversal of the impurity flux, from inward to outward, when ICRF heating is applied. However, since the ponderomotive force affects D_z and V_z in a similar way, the steady-state impurity density peaking factor $-RV_z / D_z$ is not strongly affected by the rf field.

Adding neoclassical transport will not affect the peaking factor significantly, since the effect on diffusion is negligible and the neoclassical convective velocity (for the above parameters) is smaller than the turbulent one and is inwards. Assuming large aspect ratio, circular cross-section plasma, and JET-like parameters ($n_e = 5 \times 10^{19} \text{ m}^{-3}$, $T_i = T_z = 10 \text{ keV}$, $n_z / n_e = 0.01$, $r = 0.5 \text{ m}$, and $R = 3 \text{ m}$), the neoclassical diffusion constant D_z^{neo} and convective velocity V_z^{neo} defined as $\Gamma_z^{\text{neo}} = -D_z^{\text{neo}} \nabla n_z + n_z V_z^{\text{neo}}$ are $D_z^{\text{neo}} = 0.002$ and $RV_z^{\text{neo}} = -0.34$ (in units of $2\rho_s^2 c_s / R$). Here we have assumed that both the impurities and main ions are collisionless and used Eq. (14) of Ref. 13 to calculate Γ_z^{neo} . For the parameters of Fig. 2, the inward flow due to the ion density gradient is larger than the temperature screening induced by the ion temperature gradient, and therefore the total neoclassical flow is inwards.

Figure 3 displays the impurity diffusion coefficient D_z , convective velocity RV_z , and impurity density peaking factor $-RV_z / D_z$ as a function of the ICRF ponderomotive force term $\bar{\Omega}_{i-RF}$ for a TE mode dominated case. Here, the parameters are $R/L_{Te} = 7$, $R/L_{Ti,z} = 0$, $Z = 6$, $f_i = 0.5$, $q = 1.4$, $s = 0.8$, $T_e / T_{i,z} = 1$, and $R/L_{ne} = 3$. We note that the impurity peaking factor is smaller for the TE mode dominated case: $-RV_z / D_z = 0.7$ here as compared to $-RV_z / D_z = 1.9$ for the ITG dominated case of Fig. 2 (for $\bar{\Omega}_{i-RF} = 0$). This difference is mainly a result of the parallel impurity compression term which contributes to an outward impurity convective velocity for TE modes.¹¹ We note that both D_z and V_z are reduced

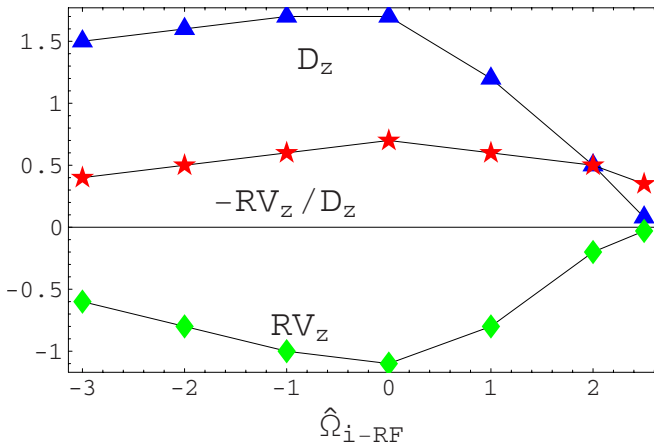


FIG. 3. (Color online) Impurity diffusion coefficient D_z , impurity convective velocity RV_z (in units of $2\rho_s^2 c_s/R$), and normalized impurity density peaking factor $-RV_z/D_z$ as a function of the ICRF ponderomotive force term $\bar{\Omega}_{i\text{-RF}}$ for a TE mode dominated case. The parameters are $R/L_{Te}=7$, $R/L_{Ti,z}=0$, $Z=6$, $f_i=0.5$, $q=1.4$, $s=0.8$, $T_e/T_{i,z}=1$, and $R/L_{ne}=3$.

regardless of the sign of $\bar{\Omega}_{i\text{-RF}}$. In this case, also the impurity peaking factor is slightly reduced in the presence of the rf field. Since the ponderomotive force terms appear explicitly only in the ion/impurity equations, the stabilization of the TE mode for these parameters is a result of the coupling to the ion physics. As in the case of Fig. 2, the neoclassical diffusion coefficient is negligibly small, but the neoclassical convective velocity is now $RV_z^{\text{neo}}=-0.67$ (in units of $2\rho_s^2 c_s/R$), assuming the same JET-like parameters as in Fig. 2), which dominates for large $\bar{\Omega}_{i\text{-RF}}$. The neoclassical inward flow is driven by the ion density gradient, and it is large, since the ion temperature gradient, which would cause an opposing outward flow, is now assumed to be zero.

In Fig. 4, the scaling of the impurity transport coefficients with ion temperature gradient R/L_{Ti} is shown. The parameters are the same as in Fig. 2, with the ponderomotive

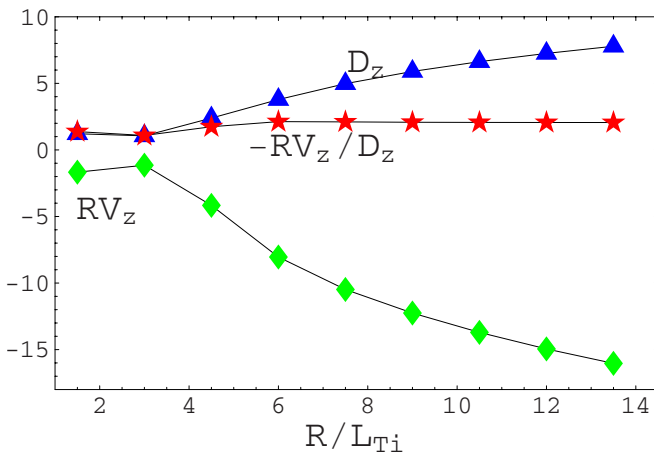
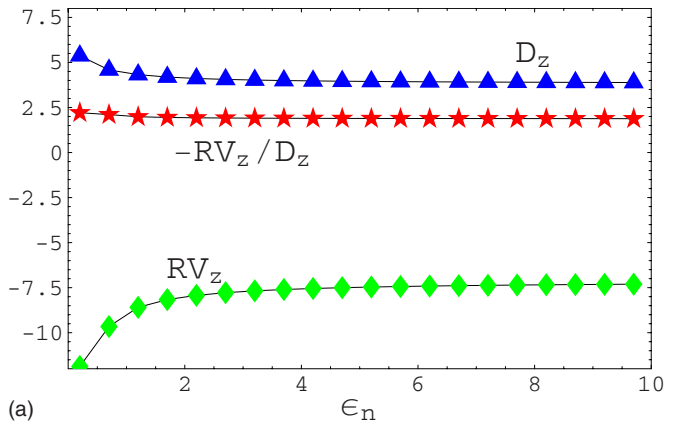
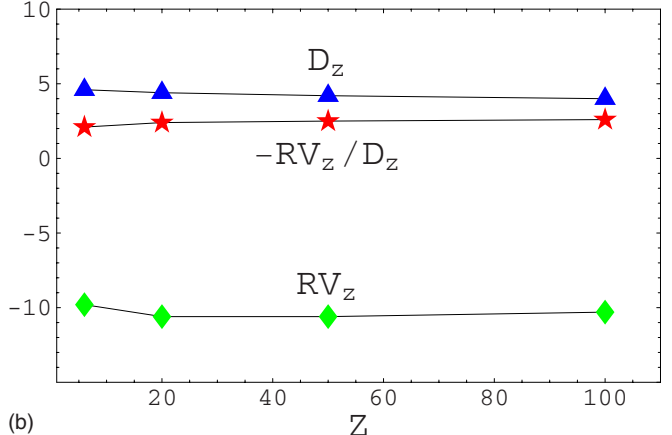


FIG. 4. (Color online) Scaling of impurity diffusion coefficient D_z , impurity convective velocity RV_z (in units of $2\rho_s^2 c_s/R$), and normalized impurity density peaking factor $-RV_z/D_z$ with ion temperature gradient R/L_{Ti} . The other parameters are the same as in Fig. 2 with $R/L_{Te}=R/L_{Tz}=7$, $Z=6$, $f_i=0.5$, $q=1.4$, $s=0.8$, $T_e/T_{i,z}=1$, and $R/L_{ne}=3$ with ponderomotive force term $\bar{\Omega}_{i\text{-RF}}=1$.



(a)



(b)

FIG. 5. (Color online) (a) Scaling of impurity diffusion coefficient D_z , impurity convective velocity RV_z (in units of $2\rho_s^2 c_s/R$), and normalized impurity density peaking factor $-RV_z/D_z$ with electron density gradient parameter $\epsilon_n=2L_n/R$. The other parameters are the same as in Fig. 2 with $R/L_{Tj}=7$, $Z=6$, $f_i=0.5$, $q=1.4$, $s=0.8$, and $T_e/T_{i,z}=1$, with ponderomotive force term $\bar{\Omega}_{i\text{-RF}}=1$. (b) Scaling of impurity diffusion coefficient D_z , impurity convective velocity RV_z (in units of $2\rho_s^2 c_s/R$), and normalized impurity density peaking factor $-RV_z/D_z$ with impurity charge Z . The other parameters are the same as in Fig. 2 with $R/L_{Tj}=7$, $R/L_{ne}=3$, $f_i=0.5$, $q=1.4$, $s=0.8$, $T_e/T_{i,z}=1$, and $A_z=2Z$, with ponderomotive force term $\bar{\Omega}_{i\text{-RF}}=1$.

force term $\bar{\Omega}_{i\text{-RF}}=1$. As observed, the onset of the ITG mode results in a large increase of D_z and $|V_z|$ as R/L_{Ti} is increased while the peaking factor $-RV_z/D_z$ increases about a factor of 2 in going from a TE dominated case (small R/L_{Ti}) to an ITG dominated case, in line with the results presented in Figs. 2 and 3. A similar change of the peaking factor can be obtained by varying the parameter T_e/T_i .

We have verified that the results presented above, in particular for the peaking factor $-RV_z/D_z$, are rather insensitive to variations in other plasma parameters. This is illustrated in Figs. 5(a) and 5(b), where parameter scalings with the electron density gradient parameter $\epsilon_n=2L_n/R$ and impurity charge Z are displayed. The other parameters are the same as in Fig. 2, with the ponderomotive force term $\bar{\Omega}_{i\text{-RF}}=1$. In Fig. 5(b), the impurity charge Z is varied from $Z=6$ to 100 and the mass of the impurity is taken as $A_z=2Z$.

IV. CONCLUSIONS

In conclusion, we have studied trace impurity transport in tokamaks due to ITG/TE mode turbulence including effects of the ponderomotive force due to an applied ICRF

field, and compared the results with neoclassical predictions. The results show that the usual inward impurity particle convective velocity and, to some extent, the impurity density peaking factor $-\nabla n_z/n_z$ can be reduced by the ponderomotive force. The effect is expected to be strongest close to the rf resonance location and is seen for both ITG and TEM dominated plasmas. The size of the anomalous convective velocity is larger than the neoclassical for typical tokamak parameter values. However, if the anomalous convection is reduced by the rf field, the neoclassical contribution may be dominant and this will modify the peaking factor. The presence of a ponderomotive force may result in a transient change of the total impurity flux, but the steady-state impurity density peaking factor $-\nabla n_z/n_z = -V_z/D_z$ does not seem to be as strongly affected by the rf field as indicated by recent tokamak experiments.⁵

¹P. Helander and D. J. Sigmar, *Collisional Transport in Magnetized Plasmas* (Cambridge University Press, Cambridge, 2002); S. P. Hirshman and D. J. Sigmar, Nucl. Fusion **21**, 1079 (1981).

²R. Dux, R. Neu, A. G. Peeters, G. Pereverzev, A. Mück, F. Ryter, and J. Stober, *Plasma Phys. Controlled Fusion* **45**, 1815 (2003).

³M. E. Puiatti, M. Valisa, M. Mattioli, T. Bolzonella, A. Bortolon, I. Coffey, R. Dux, M. von Hellermann, P. Monier-Garbet, M. F. F. Nave, and J. Ongena, *Plasma Phys. Controlled Fusion* **45**, 2011 (2003); M. F. F. Nave, J. Rapp, and T. Bolzonella, *Nucl. Fusion* **43**, 1204 (2003).

⁴M. E. Puiatti, M. Valisa, C. Angioni, L. Garzotti, P. Mantica, M. Mattioli, L. Carraro, I. Coffey, and C. Sozzi, *Phys. Plasmas* **13**, 042501 (2006).

⁵L. Carraro, C. Angioni, C. Giroud, M. E. Puiatti, M. Valisa, P. Buratti, R. Buttery, I. Coffey, L. Garzotti, D. Van Eester, L. Lauro Taroni, K. Lawson, E. Lerche, P. Mantica, M. Mattioli, and V. Naulin, in *Proceedings of the 34th EPS Conference on Controlled Fusion and Plasma Physics*, Warszawa, 2007, Vol. 31 F O 4.028.

⁶C. Giroud, C. Angioni, L. Carraro, I. H. Coffey, J. Hobirk, M. E. Puiatti, M. Valisa, A. D. Whiteford, P. Belo, T. M. Biewer, M. Brix, R. Buttery, E. Joffrin, L. Lauro Taroni, K. Lawson, P. Mantica, A. Meigs, V. Naulin, M. G. O'Mullane, and K.-D. Zastrow, in *Proceedings of 34th EPS Conference on Controlled Fusion and Plasma Physics*, Warszawa 2007, Vol. 31 F, p. 2.049.

⁷P. Gohil, L. R. Baylor, K. H. Burrell, T. A. Casper, E. J. Doyle, C. M. Greenfield, T. C. Jernigan, J. E. Kinsey, C. J. Lasnier, R. A. Moyer, M. Murakami, T. L. Rhodes, D. L. Rudakov, G. M. Staebler, G. Wang, J. G.

Watkins, W. P. West, and L. Zeng, *Plasma Phys. Controlled Fusion* **45**, 601 (2003).

⁸S. Günter, C. Angioni, M. Apostoliceanu, C. Atanasiu, M. Balden, G. Becker, W. Becker, K. Behler, K. Behringer, A. Bergmann, R. Bilato, I. Bizyukov, V. Bobkov, T. Bolzonella, D. Borba, K. Borrass, M. Brambilla, F. Braun, A. Buhler, A. Carlson, A. Chankin, J. Chen, Y. Chen, S. Cirant, G. Conway, D. Coster, T. Dannert, K. Dimova, R. Drube, R. Dux, T. Eich, K. Engelhardt, H.-U. Fahrbach, U. Fantz, L. Fattorini, M. Foley, P. Franzen, J. C. Fuchs, J. Gafert, K. Gal, G. Gantenbein, M. García Muñoz, O. Gehre, A. Geier, L. Giannone, O. Gruber, G. Haas, D. Hartmann, B. Heger, B. Heinemann, A. Herrmann, J. Hobirk, H. Hohenöcker, L. Horton, M. Huart, V. Iguchine, A. Jacchia, M. Jakobi, F. Jenko, A. Kallenbach, S. Kálvin, O. Kardaun, M. Kaufmann, A. Keller, A. Kendl, M. Kick, J.-W. Kim, K. Kirov, S. Klose, R. Kochergov, G. Kocsis, H. Kollotzek, C. Konz, W. Kraus, K. Krieger, T. Kurki-Suonio, B. Kurzan, K. Lackner, P. T. Lang, P. Lauber, M. Laux, F. Leuterer, J. Likonen, A. Lohs, A. Lorenz, R. Lorenzini, A. Lyssoivan, C. Maggi, H. Majer, K. Mank, A. Manini, M.-E. Manso, P. Mantica, M. Maraschek, P. Martin, K. F. Mast, M. Mayer, P. McCarthy, H. Meyer, D. Meisel, H. Meister, S. Menmuir, F. Meo, P. Merkel, R. Merkel, D. Merkl, V. Mertens, F. Monaco, A. Mück, H. W. Müller, M. Münich, H. Murmann, Y.-S. Na, R. Narayanan, G. Neu, R. Neu, J. Neuhauser, D. Nishijima, Y. Nishimura, J.-M. Noterdaeme, I. Nunes, M. Pacco-Düchs, G. Pautasso, A. G. Peeters, G. Pereverzev, S. Pinches, E. Poli, E. Posthumus-Wolfrum, T. Pütterich, R. Pugno, E. Quigley, I. Radivojevic, G. Raupp, M. Reich, R. Riedl, T. Ribeiro, V. Rohde, J. Roth, F. Ryter, S. Saarelma, W. Sandmann, J. Santos, G. Schall, H.-B. Schilling, J. Schirmer, W. Schneider, G. Schramm, J. Schweinzer, S. Schweizer, B. Scott, U. Seidel, F. Serra, C. Sihler, A. Silva, A. Sips, E. Speth, A. Stäbler, K.-H. Steuer, J. Stober, B. Streibl, D. Strintzi, E. Strumberger, W. Suttorp, G. Tardini, C. Tichmann, W. Treutterer, M. Troppmann, M. Tsallas, H. Urano, P. Varela, D. Wagner, F. Wesner, E. Würsching, M. Y. Ye, S.-W. Yoon, Q. Yu, B. Zaniol, D. Zasche, T. Zehetbauer, H.-P. Zehrfeld, M. Zilker, and H. Zohm, *Nucl. Fusion* **45**, S98 (2005).

⁹J. Luxon, *Nucl. Fusion* **42**, 614 (2002).

¹⁰P. H. Rebut, Nucl. Fusion **25**, 1011 (1985).

¹¹C. Angioni and A. G. Peeters, *Phys. Rev. Lett.* **96**, 095003 (2006).

¹²J. Weiland, *Collective Modes in Inhomogeneous Plasma* (IOP, Bristol, 2000).

¹³H. Nordman, T. Fülöp, J. Candy, P. Strand, and J. Weiland, *Phys. Plasmas* **14**, 052303 (2007).

¹⁴T. Hellsten and L. Villard, Nucl. Fusion **28**, 285 (1988).

¹⁵R. J. Dumont and L.-G. Eriksson, *AIP Conf. Proc.* **871**, 65 (2006).

¹⁶A. Sen, P. K. Kaw, and A. K. Sundaram, in *Proceedings of the 11th Conference on Plasma Physics and Controlled Nuclear Fusion* (IAEA, Kyoto, Japan, 1986).

¹⁷A. Hirose, *Phys. Fluids B* **5**, 230 (1993).